

Vision Transformers for End-to-End Vision-Based Quadrotor Obstacle Avoidance

Anish Bhattacharya^{*,1}, Nishanth Rao^{*,1}, Dhruv Parikh^{*,1}, Pratik Kunapuli¹, Nikolai Matni¹, and Vijay Kumar¹

Abstract—We demonstrate the capabilities of an attention-based end-to-end approach for high-speed quadrotor obstacle avoidance in dense, cluttered environments, with comparison to various state-of-the-art architectures. Quadrotor unmanned aerial vehicles (UAVs) have tremendous maneuverability when flown fast; however, as flight speed increases, traditional vision-based navigation via independent mapping, planning, and control modules breaks down due to increased sensor noise, compounding errors, and increased processing latency. Thus, learning-based, end-to-end planning and control networks have shown to be effective for online control of these fast robots through cluttered environments. We train and compare convolutional, U-Net, and recurrent architectures against vision transformer models for depth-based end-to-end control, in a photorealistic, high-physics-fidelity simulator as well as in hardware, and observe that the attention-based models are more effective as quadrotor speeds increase, while recurrent models with many layers provide smoother commands at lower speeds. To the best of our knowledge, this is the first work to utilize vision transformers for end-to-end vision-based quadrotor control.

I. INTRODUCTION

Quadrotor unmanned aerial vehicles (UAVs) are small, agile vehicles that can fly with high levels of acceleration and agility. With the miniaturization of onboard sensing and computing, it is now common to treat quadrotors as a single, independent robot that senses its environment, performs high level planning, calculates low level control commands, then tracks these commands using an onboard-calculated state estimate. Prior to recent work, most research in this field has been done with the traditional robotics pipeline of individual and modular sensing, planning, and control blocks, each with some computational requirements and error tolerances. However, quadrotors reach their highest utility when flown fast, thereby achieving more coverage with limited battery life; at these speeds, perception-to-planning via the modular approach can break down [1]. Recent works have explored using learned policies to develop a single sensing-to-planning algorithm that feeds into a tracking controller; this has fast reaction times and generalizes to sensor noise and real-world artifacts when learned models are trained with domain randomization techniques [2]. In contrast, we explore a full end-to-end approach, encapsulating more of the tracking task into a vision transformer (ViT) model.

We aim to explore the utility of attention-based learning models, specifically vision transformer architectures that take

images as input, for end-to-end control of a quadrotor for the high-speed obstacle avoidance task. We adopt the task and simulator from the ICRA 2022 DodgeDrone Challenge: Vision-based Agile Drone Flight, showcasing various teams' efforts to develop obstacle avoidance policies for a quadrotor flying through a cluttered simulation environment. Against our chosen ViT architecture, we select as baselines a range of learning backbones that have varying use-cases: convolutional network, U-Net network, and recurrent network. While this is not an exhaustive list of all popular learning architectures available today, we believe this covers a wide range of model types typically used for vision-based-control related tasks, including object detection, image segmentation, and temporal sequence modeling.

The favorable qualities of convolutional networks [3, 4] have driven much of the work in vision-based UAV control. These networks are able to learn feature maps that, when trained with gradients computed relative to a desired objective function, outperform hand-engineered feature maps and additionally are translationally invariant. However, when used for the control of dynamical systems, they do not maintain any internal state and thus do not have any memory of past states or actions. In robotics tasks where both the robot and thus the sensory input are dynamic, it has yet to be shown that convolutional networks are the best method for perception. Recurrent architectures (e.g., long short term memory [5]) are models that maintain an internal state and may provide smoother, more feasible commands to dynamic robots such as quadrotors [6]. More recent sequence modeling techniques use the attention mechanism [7] to construct transformers [8] that have been adapted from the natural language processing domain for vision [9] and show superior performance in object recognition and tracking. These vision transformers take as input the patches of an image as a sequence, and when provided with large training datasets, outperform convolutional or recurrent networks in a growing number of computer vision tasks. Further motivation lies in prior work which suggests that using recurrent or attention-based models might improve performance due to the temporal nature of dynamic robot navigation [10].

This work's aim is to study the ViT as an end-to-end framework for quadrotor control, with comparisons to baseline models. As such, we choose behavior cloning from an obstacle-aware expert as the learning paradigm, as is common among existing learning-to-fly works [2, 11]. This additionally eliminates potentially confounding factors that may exist in a reinforcement learning framework, such as the exploration/exploitation tradeoff and additional hy-

^{*}Equal contribution.

¹The General Robotics, Automation, Sensing & Perception (GRASP) Lab, University of Pennsylvania, 3330 Walnut St, Philadelphia, PA 19104, United States. Corresponding author: anish1@seas.upenn.edu.

perparameter tuning. We use depth sensing data to train and evaluate these models, as across multiple sensor types, robotic platforms, and environments, depth data has shown in prior work to be both ubiquitous and effective at high-level scene understanding as well as navigation tasks. We evaluate models against each other by comparing collision metrics and success rates during forward flight through a cluttered scene, with increasing forward velocities. We also present the paths taken by each model, as well as the command characteristics (acceleration and energy cost).

Our contributions are as follows:

- The first use of vision transformer models for high-speed end-to-end control of a quadrotor.
- A comparison of a vision transformer model against various state-of-the-art learning-based models for end-to-end depth-based control of quadrotors.
- Real experiments demonstrating and comparing models on hardware.
- Open-source code and datasets to reproduce and extend results in this paper.¹

II. RELATED WORK

End-to-end vision-based navigation. End-to-end approaches for control tasks have been investigated in a variety of settings such as autonomous driving [12], and partially so in autonomous quadrotor flight in the wild [2]. Both works demonstrate that such approaches have high sample complexity, and in the more structured self-driving task, it does not generalize as well as modular approaches. However, both end-to-end and structured methods degrade in performance as agility increases. Existing works for learned end-to-end quadrotor flight largely focus on flight at a relatively slow speed and use raw images directly [11, 13].

Vision transformers for control. Some research has used a combination of architectures to surpass the performance of individual components for the object detection task. Swin Transformer [14] and a ResNet-based module [15] have been combined previously [16], showing that this attention+convolutional network architecture improved object detection performance. We similarly explore combination models between basic backbone architectures (convolution and U-Net, recurrence, and attention) in this work. When looking at downstream tasks such as control from pixels, transformer architectures such as ViT have been compared to convolutional neural networks (CNNs) and shown to perform worse than the CNN architecture due to the weaker inductive bias and need for more training data [17, 18]. ViT has been studied extensively for its use in downstream control tasks as a representation learner in many reinforcement learning (RL) works [19–21]. Our method investigates leveraging similar architectures using imitation learning from a privileged expert as opposed to RL.

Vision transformers with quadrotors. Since the development of the ViT, some works have used such models with onboard imagery from quadrotors but not in the same module

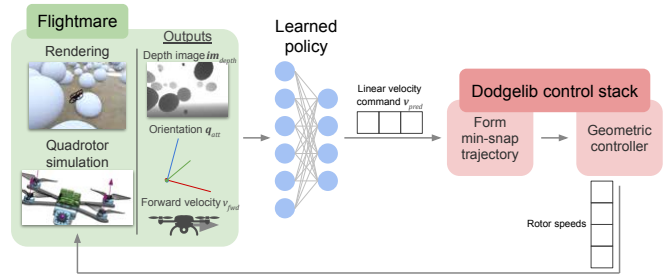


Fig. 1: Depth images \mathbf{im}_{depth} and quadrotor orientation \mathbf{q}_{att} come from Flightmare, and along with forward velocity v_{fwd} serve as input to the chosen learning model. The model outputs a linear velocity command \mathbf{v}_{pred} which leads to the formation of a min-snap trajectory that is followed by a geometric controller, both part of the Dodgelib control stack [27]. This outputs rotor speeds, which is sent to the quadrotor simulator in Flightmare.

used for planning or control. Some perform object detection onboard a UAV [22, 23]. Object tracking and then servoing has been attempted in the past, where a Siamese Transformer Network performs object tracking onboard a UAV, then independently a PD visual servoing algorithm commands yaw angle and forward velocity from the bounding box [24]. To our knowledge, our work represents the first investigation for using ViT in an end-to-end manner with quadrotor control.

Quadrotor flight from depth images. When navigating in uncertain environments, learning from depth images offers an input modality for reactive control [2, 25, 26]. Various approaches have been taken to learn control outputs from depth image inputs such as mapping then planning [25], using motion primitives [26], and sampling collision-free trajectories [2]. These methods use depth images to determine some intermediate representation which is then used to control the quadrotor. Compared to these methods, we demonstrate purely end-to-end control using various architectures learning from depth images directly, without the need for mapping, planning, or trajectory generation.

III. METHODOLOGY

A. Task Formulation

We formulate the obstacle avoidance task as flying forward a fixed distance at various forward velocities while avoiding static, spherical obstacles in a simulated, cluttered environment that is unstructured and unknown. The expert is a reactive planner that was designed to be short-sighted and mimic data available to low-skill pilots, thereby avoiding real-world, high-risk, in-situ training and not relying on trained-pilot data that might be close to time-optimal but expensive. Supervisory data is collected during expert policy rollouts to train the end-to-end learning-based student models. As this work aims to study ViTs against other models for developing reactive obstacle avoidance behavior, all models output linear velocity commands in the world frame, in contrast to long-horizon trajectory planning often used for less reactive policies in prior work [2]. To assess model performance, we consider multiple obstacle collision metrics,

¹www.anishbhattacharya.com/research/vit-depthfly

computational complexity and inference time, among other quantitative and qualitative factors.

Formally, we consider an obstacle-aware expert $\pi_{\text{expert}}(s_t, o) = a_t$ which takes as input quadrotor state s_t , obstacle locations o , and produces action a_t at every timestep t . A dataset \mathcal{D} is collected by conducting many trajectories τ under which the transition dynamics \mathcal{T} are produced under the expert $s_{t+1} = \mathcal{T}(s_t, a_t)$, $a_t \sim \pi_{\text{expert}}(s_t, o)$ and the depth image $\mathbf{im}_{\text{depth},t}$ is recorded at every timestep. We then seek to train a student policy $\pi_{\text{student}}(s_t, \mathbf{im}_{\text{depth},t}) = a_t$ which is not directly aware of obstacle locations but instead relies on depth images to reproduce the actions of the expert policy (1).

B. Learning framework

The student model takes as input a single depth image $\mathbf{im}_{\text{depth}} \in [0, 1]^{60 \times 90}$ (similar to [2]) of size 60×90 , quadrotor attitude $\mathbf{q}_{\text{att}} = (w, x, y, z)$, and forward velocity $v_{\text{fwd}} \in \mathbb{R}$, and predicts a velocity vector $\mathbf{v}_{\text{pred}} \in \mathbb{R}^3$. As models have access to the forward velocity, we do not include other variations of model inputs such as image sequences; while this input might improve temporal predictions of convolution-only models, we instead present recurrent models that are meant to model sequences. The v_{pred} are learned from a privileged expert in a supervised behavior cloning fashion, with a standard L2 loss over all timesteps in a trajectory, given student model parameters θ .

$$L(\theta) = \mathbb{E}_{\tau \sim \mathcal{D}} \left[\frac{1}{T} \sum_{t=0}^{T-1} \|v_{\text{cmd}}(t) - v_{\text{pred}}(t; \theta)\|_2^2 \right] \quad (1)$$

C. Simulated setup and models

Simulation and rendering. We use the open-source Flightmare simulator [28] that contains fast physics simulations of quadrotor dynamics and a bridge to the high-visual-fidelity game engine renderer Unity. In addition to being ROS-enabled, this simulator package allows us to collect training data from and deploy quadrotors in various environments with accurate depth sensor measurements with real-time computations on a laptop computer. Specifically, we use a modified version of the simulator supplied for the DodgeDrone ICRA 2022 Competition [27] which contains an environment with floating spherical obstacles of various sizes (later referred to as ‘‘spheres environment’’). The simulated Kingfisher model quadrotor has a mass of 0.752kg and a diameter of 0.25m.

Privileged expert policy and data gathering. To gather supervisory data pairs of $\{(\mathbf{im}_{\text{depth}}, \mathbf{q}_{\text{att}}, v_{\text{fwd}}), \mathbf{v}_{\text{pred}}\}$ for behavior cloning, a privileged expert runs its collision avoidance algorithm through randomized obstacle fields. Note that bold variables are multi-dimensional. In total, 588 expert runs yielded 112k depth images, where 27.5k images are sampled from trials where there is at least one collision. Since the expert is reactive and lacks dynamics-feasible planning, collisions are not uncommon; however, we find that some models (see Section IV-A) outperform this expert at high speeds.

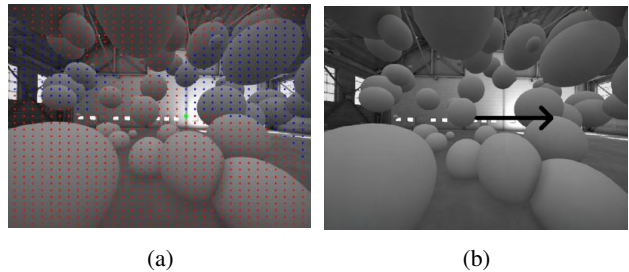


Fig. 2: Expert policy visualized from the quadrotor onboard camera in sample training environment. (a) Visualization of obstacle collision information along a waypoint grid, where blue dots represent straight-line paths in free space, red dots are in collision, and the green is the chosen flight path direction; (b) the black arrow shows the current commanded velocity direction and magnitude.

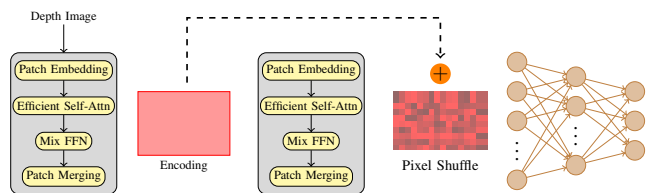


Fig. 3: ViT model used in this study. ViT+LSTM uses a multi-layer LSTM placed before the final FC layers.

The privileged expert can access obstacle position and radius information o of those obstacles within 10m of the current drone position $s_{t,\text{pos}}$. It searches for straight-line collision-free trajectories from the drone’s current position to each waypoint along a 2D grid in the lateral-vertical plane set at some horizon ahead of the drone, as demonstrated in Figure 2. The waypoint closest to the center of the grid is chosen, and a gain is applied to this relative position to generate a velocity command action a_t . Transition dynamics \mathcal{T} are provided by the Flightmare quadrotor simulation.

End-to-end student models. We present five student models for a comparison of ViT-based models against other state-of-the-art architecture types for processing image data. Each model takes as initial input a single depth image, and uses an encoder-shape module first (convolutional layers or attention layers) to generate a lower-dimensional middle representation that is then concatenated with the quadrotor attitude (quaternion) and forward velocity (scalar) before feeding into either LSTM or fully-connected layers. With the exception of the ConvNet model, all models are roughly 3M parameters (Table I) for a fair comparison. This model size ensures fast enough computation for in-flight processing in a robotics control loop (30Hz on the hardware platform presented in Section III-D). Certain models such as a fully transformer-based architecture were attempted, but performed poorly and are not presented (unless a fully-connected head was used, as is described below as ViT).

ViT. We utilize a transformer based encoder inspired by Segformer [29], and apply two transformer blocks in hierarchical fashion, followed by upsampling using pixel shuffle [30], and mixing of information across hierarchies

Model	Trainable parameters	CPU (ms)	GPU (ms)
ConvNet	235,269	0.195	0.423
LSTMnet	2,949,937	4.75	0.735
UNet+LSTM	2,955,822	5.56	1.67
ViT	3,101,199	5.58	3.83
ViT+LSTM	3,563,663	9.16	1.61

TABLE I: Model size and inference times per model. Times are presented from a 12th Gen Intel i7-12700H CPU and Nvidia GeForce RTX 3060 GPU, with benchmark times obtained using TorchBench [31] via 1000 single-threaded iterations.

Model	Structure		Components		
	UNet	ViT	Conv	LSTM	MLP
ConvNet	✗	✗	✓(2)	✗	✓(4)
LSTMnet	✗	✗	✓(2)	✓(2)	✓(3)
UNet+LSTM	✓	✗	✓(2)	✓(2)	✓(3)
ViT	✗	✓	✓(1)	✗	✓(3)
ViT+LSTM	✗	✓	✓(1)	✓(3)	✓(2)

TABLE II: Structure and layer components per model. ConvNet and LSTMnet are structured by the rudimentary layer types themselves. Numbers next to checkmarks indicate how many layers of that type are present in the model.

using a convolution operation. This incorporates information at multiple scales. This ViT is followed by fully connected layers. This very lightweight architecture is presented in Figure 3.

ViT+LSTM. This is identical to the ViT model but includes a multi-layer LSTM before the fully connected layers.

ConvNet. A lightweight CNN model that resembles the first successful deep-learning-based approaches for object detection or end-to-end vision-based control for robots. This model is considered a control model, and is the only one significantly smaller than 3M parameters. ResNet-18 [15], a large CNN model that learns residuals from the input signal, was also trained and tested but found to perform similarly to the ConvNet model and worse than the UNet model, demonstrating that simply increasing the number of parameters in the ConvNet does not lead to better performance.

ConvNet+LSTM. A multi-layer LSTM module placed between the convolutional and fully connected layers is included to encourage temporal consistency in velocity predictions.

UNet+LSTM. The symmetric encoder-decoder architecture popular in segmentation tasks includes skip connections that incorporate local and global information and help prevent vanishing gradients. The reduction to a lower-dimensional feature space also may improve generalizability to unseen environments. A multi-layer LSTM follows the UNet.

D. Hardware setup

We use the Falcon 250 custom quadrotor platform [32] (Figure 10a) running the `kr_mav_control` [33] open-source quadrotor control stack. All experiments are performed in a Vicon motion capture arena for accurate state estimate. The Intel Realsense D435i depth camera utilizes both structured light via an infrared emitter and stereo matching to calculate depth images. These images are resized to match the simulation-size images, then fed directly into the

network models. The output velocity command is sent to the control stack, which outputs a SO(3) command (orientation and thrust) that is sent to the PX4 controller [34]. While we train models on floating objects in simulation, we test with a single, self-standing object in the real-world.

IV. RESULTS

A. Collision metrics and success rates

We assess models with two metrics quantifying collisions over multiple trials in different, unseen sphere environments in Figure 4; generalization performance is detailed in Section IV-D. Average collision rate describes the number of collisions per trial, and mean time spent in collision counts the time the drone spent in collision with obstacles. Impacts with large obstacles and head-on collisions tend to increase the values of the second metric. Figure 4a shows that the average number of collisions per trial generally increases as a function of velocity for every model, as expected due to lower allowed response time and as shown in prior work. However, the ViT+LSTM begins to outperform the expert as speeds increase beyond 5m/s. ConvNet presents similar behavior until 6m/s. As the training dataset included expert trajectories with collisions, it is notable that the ViT+LSTM model outperforms this expert. Furthermore, the models primarily composed of the individual components of the ViT+LSTM model, namely ViT and LSTMnet, do not perform well, while the combination model maintains a significantly lower collision rate as speeds reach 7m/s.

Expert mean time in collision (Figure 4b) is particularly bad since each collision caused the waypoint search to fail; however, notably, the poor expert statistics are not learned by any of the models. The ViT+LSTM model outperforms all other models in this metric as well, especially as speeds increase. By observation, the ViT+LSTM model tends to clip the edges of obstacles and have fewer head-on collisions than other models; this results in fewer timesteps spent in collision.

B. Path and command characteristics

The trajectory paths in Figure 5 exhibit the paths of each model as the drone flies from the $x = 0$ starting point to $x = 60$. The ConvNet demonstrates significantly less variation in paths, while the ViT model exhibits changing spread in chosen paths as it progresses through the obstacle field. In contrast, the ViT+LSTM model has a steadily increasing spread as x position increases, possibly suggesting both a balance between model capacity as well as consistency of commands over multiple trials, though this needs further investigation.

Figure 6 presents command characteristics of each model across forward velocities in the spheres environment test set. We observe that smoother velocity commands are more feasible to track by the quadrotor and result in lower commanded acceleration, and the energy cost metric is computed as in [35]. The ViT model has high commanded accelerations across all forward velocities, but this is drastically improved with the addition of the LSTM layers for ViT+LSTM;

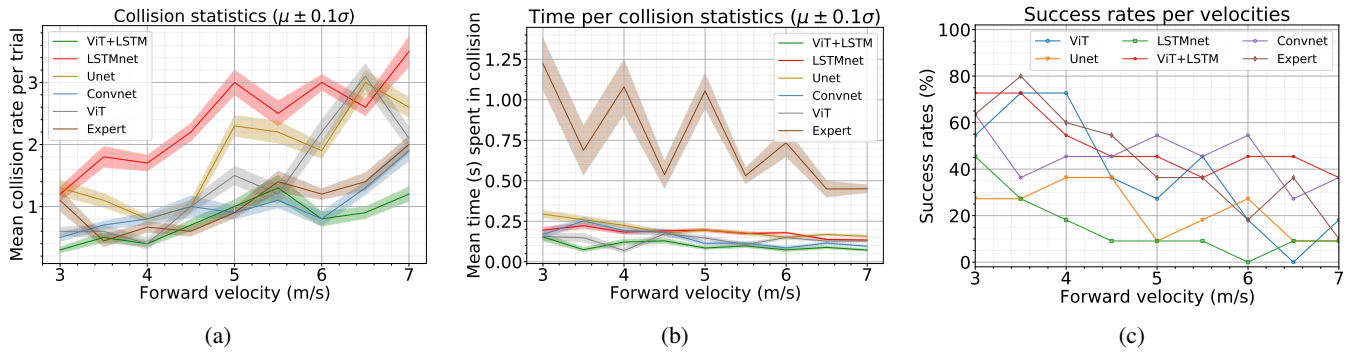


Fig. 4: Collision and success metrics for each model, taken over 10 randomized, unseen simulation sphere configuration trials at each forward velocity. (a) Mean number of collisions per trial. Most models do not outperform the expert up to speeds of 5m/s, beyond which the ViT+LSTM model outperforms both the expert and other models. (b) Mean time spent in collision per trial, with each trial lasting between 8.5-20s. This metric tends to increase with collision “severity”, i.e. head-on collisions and large-obstacle collisions. The models outperform the expert, and ViT+LSTM does the best. (c) Success rates, i.e. the fraction of trials containing no collisions. ConvNet and ViT+LSTM are the most consistent models with forward velocity.

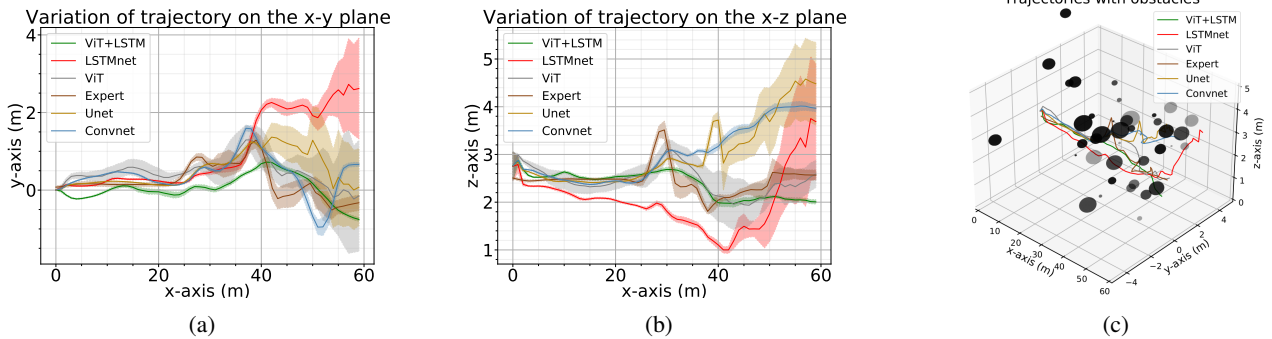


Fig. 5: Visualizing the trajectories taken by each model in a single test environment over multiple trials. (a) Top-down view with 0.1σ distribution of the mean position, (b) side-view with 0.1σ distribution of the mean position, (c) 3D perspective of the mean paths.

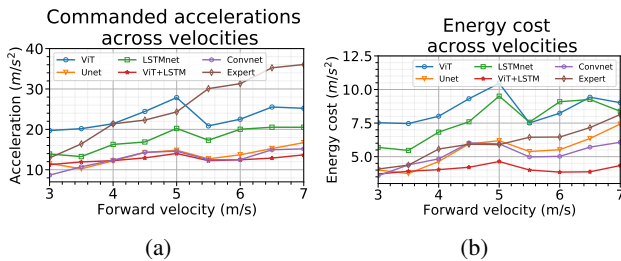


Fig. 6: Commanded accelerations (a) and computed energy costs (b) for all models in the spheres environment. Lower is considered better for both metrics. The ViT-only model commands high-acceleration values without achieving better performance, but the inclusion of recurrent layers improves this behavior.

notably this comes without a drop in performance (Figure 4). Generally, models including recurrent (LSTM) components command lower acceleration and have lower energy cost; this is particularly the case in the trees environment (Figure 8c) described in Section IV-D.

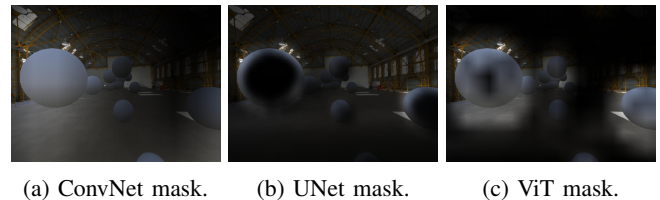


Fig. 7: Mask visualizations for each spatial operation used in this comparison study. Color images are shown for viewability, though aligned *depth* images are used as input to the models. ConvNet generally highlights entire obstacles, while UNet and ViT highlights edges. ViT seems to additionally capture more context around obstacles.

C. Network feature analysis

Figure 7 highlights areas of the depth image that return the strongest signal by the convolutional layers in the ConvNet model and UNet model, and that of the attention layers in the ViT model. Convnet highlights full obstacles, with little specificity to their shape. UNet layers specifically highlight the edges and disregard all other areas of the image. The ViT model seems to both capture obstacle edges and surrounding

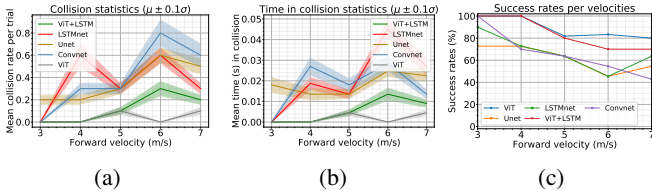


Fig. 8: Generalization to trees: collision and success metrics for each model, taken over 10 randomized tree environments. Since we did not train on trees, we do not compare with the expert. (a) Mean number of collisions per trial. (b) Mean time spent in collision per trial. (c) Success rates, i.e. the fraction of trials containing no collisions.

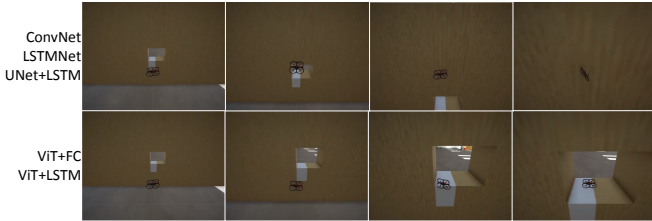


Fig. 9: Demonstration of paths taken by non-ViT and ViT models for the simulated flying through a window task. Only the ViT-based models succeed at this challenging task. One representative example is shown for each category since the models within both categories perform similarly.

context, likely a result of the known behavior of ViTs to learn relationships between parts of an image in prior object detection work [9].

D. Generalizability

To test model generalization capabilities, we zero-shot deploy the models in a simulation environment containing realistic looking tree models placed randomly in the scene (“tree environment”). We present collision rates and success rates in Figure 8 that resemble the in-distribution sphere environment testing results, showing that the ViT and ViT+LSTM models generalized well and outperformed other models. As speeds increase to 5m/s, time spent in collision increases in this particular environment, suggesting that collisions are more head-on when they occur for such models.

We additionally present a zero-shot fly-through-window experiment performed across all models at 3 m/s (Figure 9). While the spheres and trees environment contains obstacles within free space, with multiple viable collision-free paths, this environment is completely in collision except for one viable collision-free path. Only the ViT models (ViT and ViT+LSTM) succeed at this task, and all others fail. This presents additional evidence that ViT models are superior in generalization compared to other state-of-the-art computer vision models, including recurrent models, for end-to-end quadrotor control.

E. Ablation against state information

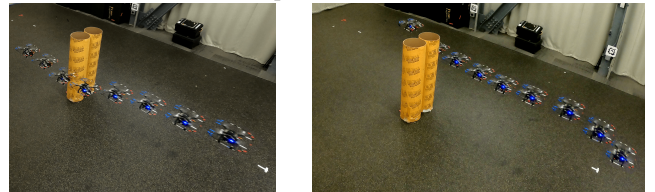
We perform an ablation against the included state information of quadrotor orientation and forward velocity by training and testing the models without this data (therefore the only input is the depth image itself), with success rates presented

Env	Models	Velocity (m/s)					
		3		5		7	
		✓	✗	✓	✗	✓	✗
Spheres	ViT	54	81	27	18	18	18
	ViT+LSTM	72	54	45	45	36	9
	Convnet	63	27	54	18	36	10
	LSTMnet	45	27	9	18	9	9
	Unet	27	36	9	18	9	27
Trees	ViT	100	90	81	81	80	81
	ViT+LSTM	100	90	80	81	70	50
	Convnet	100	90	63	81	42	60
	LSTMnet	90	90	63	40	63	36
	Unet	72	100	63	60	54	45

TABLE III: Success rates (%) for each model with quadrotor attitude and forward velocity included (✓) or not (✗) for the spheres and trees environments. ViT+LSTM and ConvNet suffer the most from lack of this data.



(a) Falcon 250 custom quadrotor platform with a 402mm tip-to-tip diameter, an Intel Realsense D435 depth camera, a Pixhawk 4 Mini flight controller, and an Intel NUC 10 onboard computer with a i7-10710U CPU. Inference is performed onboard.



(b) ConvNet trial.

(c) ViT+LSTM trial.

Fig. 10: Real world experiments evaluating the ConvNet and ViT+LSTM models in a dodging task against a rigid obstacle.

in Table III. This ablation is particularly relevant since flying in the wild may result in noisy state estimates and variable forward velocities. The results show that ViT+LSTM suffered from lack of this information as speeds increased beyond 5m/s, and the ConvNet model suffered across all speeds in the spheres environment. In the tree environment, at low speeds most models either maintained or improved success rates when lacking this data. As speeds increase, ConvNet performs better in this unseen, generalization environment without the data.

F. Hardware demonstrations

We zero-shot deploy the two most successful and most different models from simulation, ConvNet and ViT+LSTM, onboard the Falcon 250 hardware platform described in Section III-D and observe the path of the drone while it dodges a single object. Figure 10 shows the stark difference in paths taken, which we observed to be consistent over multiple trials. The ConvNet does not begin the dodging maneuver until very late (<1m distance to obstacle), and then dodges very closely to the obstacle. The ViT+LSTM, however, begins the dodging maneuver much earlier (2m distance to obstacle) and proceeds to take a wide path around the obstacle. While further analysis is needed, these results

suggest that the ViT+LSTM model has benefits over a simple ConvNet-style model for real-world deployment.

V. CONCLUSION

We present the use of a vision transformer for end-to-end obstacle avoidance of a quadrotor from depth perception, and compare it to other popular learning-based architectures. All models were trained in the same fashion from a privileged expert via behavior cloning. Models with significant recurrent layers command lower accelerations with lower energy cost but low success rates, while ViT attention-based models *without* an LSTM layer command high values but have higher success rates. The attention-recurrent (ViT+LSTM) model, however, has desirably low acceleration and energy cost while presenting the best collision and success rates. The attention-based models drastically outperformed all other models in simulated generalization tests of a trees environment and a challenging flying-through-window task. Real world demonstrations show that the attention-recurrent (ViT+LSTM) combination model actuates to dodge much earlier than the convolution-only (ConvNet) model, and analyzing model layer masks suggests that attention layers capture context around obstacles in addition to highlighting the edges of visible obstacles. Further work might explore how sensor noise, poor state estimate, and varying robotic platforms may affect generalization capabilities of these end-to-end models. Additionally, commanding lower-level control commands such as collective-thrust and body-rates (CTBR) might outperform commands of linear velocities when attempting learned, fast and agile flight.

ACKNOWLEDGMENT

We thank members of the Kumar Robotics Lab for their help with hardware experiments, rich research discussions, and generous support. This work was funded by NSF SLES-2331880 and NSF CAREER-2045834.

REFERENCES

- [1] Davide Falanga, Suseong Kim, and Davide Scaramuzza. “How fast is too fast? the role of perception latency in high-speed sense and avoid”. In: *IEEE Robotics and Automation Letters* 4.2 (2019), pp. 1884–1891.
- [2] Antonio Loquercio, Elia Kaufmann, René Ranftl, Matthias Müller, Vladlen Koltun, and Davide Scaramuzza. “Learning high-speed flight in the wild”. In: *Science Robotics* 6.59 (Oct. 2021). ISSN: 2470-9476.
- [3] Yann LeCun, Bernhard Boser, John Denker, Donnie Henderson, Richard Howard, Wayne Hubbard, and Lawrence Jackel. “Handwritten digit recognition with a back-propagation network”. In: *Advances in neural information processing systems* 2 (1989).
- [4] Pierre Sermanet, Soumith Chintala, and Yann LeCun. “Convolutional neural networks applied to house numbers digit classification”. In: *Proceedings of the 21st international conference on pattern recognition (ICPR2012)*. IEEE. 2012, pp. 3288–3291.
- [5] Sepp Hochreiter and Jürgen Schmidhuber. “Long short-term memory”. In: *Neural computation* 9.8 (1997), pp. 1735–1780.
- [6] Jiajun Ou, Xiao Guo, Ming Zhu, and Wenjie Lou. “Autonomous quadrotor obstacle avoidance based on dueling double deep recurrent Q-learning with monocular vision”. In: *Neurocomputing* 441 (2021), pp. 300–310.
- [7] Dzmitry Bahdanau, Kyunghyun Cho, and Yoshua Bengio. “Neural machine translation by jointly learning to align and translate”. In: *arXiv preprint arXiv:1409.0473* (2014).
- [8] Ashish Vaswani, Noam Shazeer, Niki Parmar, Jakob Uszkoreit, Llion Jones, Aidan N Gomez, Łukasz Kaiser, and Illia Polosukhin. “Attention is all you need”. In: *Advances in neural information processing systems* 30 (2017).
- [9] Alexey Dosovitskiy, Lucas Beyer, Alexander Kolesnikov, Dirk Weissenborn, Xiaohua Zhai, Thomas Unterthiner, Mostafa Dehghani, Matthias Minderer, Georg Heigold, Sylvain Gelly, et al. “An image is worth 16x16 words: Transformers for image recognition at scale”. In: *arXiv preprint arXiv:2010.11929* (2020).
- [10] Yunlong Song, Kexin Shi, Robert Penicka, and Davide Scaramuzza. “Learning perception-aware agile flight in cluttered environments”. In: *2023 IEEE International Conference on Robotics and Automation (ICRA)*. IEEE. 2023, pp. 1989–1995.
- [11] Antonio Loquercio, Ana I Maqueda, Carlos R DelBlanco, and Davide Scaramuzza. “Dronet: Learning to fly by driving”. In: *IEEE Robotics and Automation Letters* 3.2 (2018), pp. 1088–1095.
- [12] Matthias Mueller, Alexey Dosovitskiy, Bernard Ghanem, and Vladlen Koltun. “Driving Policy Transfer via Modularity and Abstraction”. In: *Proceedings of The 2nd Conference on Robot Learning*. Ed. by Aude Billard, Anca Dragan, Jan Peters, and Jun Morimoto. Vol. 87. Proceedings of Machine Learning Research. PMLR, 2018, pp. 1–15. URL: <https://proceedings.mlr.press/v87/mueller18a.html>.
- [13] Xi Dai, Yuxin Mao, Tianpeng Huang, Na Qin, Deqing Huang, and Yanan Li. “Automatic obstacle avoidance of quadrotor UAV via CNN-based learning”. In: *Neurocomputing* 402 (2020), pp. 346–358.
- [14] Ze Liu, Yutong Lin, Yue Cao, Han Hu, Yixuan Wei, Zheng Zhang, Stephen Lin, and Baining Guo. “Swin transformer: Hierarchical vision transformer using shifted windows”. In: *Proceedings of the IEEE/CVF international conference on computer vision*. 2021, pp. 10012–10022.
- [15] Kaiming He, Xiangyu Zhang, Shaoqing Ren, and Jian Sun. “Deep residual learning for image recognition”. In: *Proceedings of the IEEE conference on computer vision and pattern recognition*. 2016, pp. 770–778.

- [16] Willy Fitra Hendria, Quang Thinh Phan, Fikriansyah Adzaka, and Cheol Jeong. "Combining transformer and CNN for object detection in UAV imagery". In: *ICT Express* 9.2 (2023), pp. 258–263.
- [17] Tianxin Tao, Daniele Reda, and Michiel van de Panne. *Evaluating Vision Transformer Methods for Deep Reinforcement Learning from Pixels*. 2022. arXiv: 2204.04905 [cs.LG].
- [18] Wenzhe Li, Hao Luo, Zichuan Lin, Chongjie Zhang, Zongqing Lu, and Deheng Ye. "A Survey on Transformers in Reinforcement Learning". In: *Transactions on Machine Learning Research* (2023). Survey Certification. ISSN: 2835-8856.
- [19] Nicklas Hansen, Hao Su, and Xiaolong Wang. "Stabilizing deep q-learning with convnets and vision transformers under data augmentation". In: *Advances in neural information processing systems* 34 (2021), pp. 3680–3693.
- [20] Amir Ardalan Kalantari, Mohammad Amini, Sarah Chandar, and Doina Precup. "Improving sample efficiency of value based models using attention and vision transformers". In: *arXiv preprint arXiv:2202.00710* (2022).
- [21] Younggyo Seo, Danijar Hafner, Hao Liu, Fangchen Liu, Stephen James, Kimin Lee, and Pieter Abbeel. "Masked world models for visual control". In: *Conference on Robot Learning*. PMLR. 2023, pp. 1332–1344.
- [22] Reenul Reedha, Eric Dericquebourg, Raphael Canals, and Adel Hafiane. "Transformer neural network for weed and crop classification of high resolution UAV images". In: *Remote Sensing* 14.3 (2022), p. 592.
- [23] Tao Ye, Wenyang Qin, Zongyang Zhao, Xiaozhi Gao, Xiangpeng Deng, and Yu Ouyang. "Real-Time Object Detection Network in UAV-Vision Based on CNN and Transformer". In: *IEEE Transactions on Instrumentation and Measurement* 72 (2023), pp. 1–13.
- [24] Xiaolou Sun, Qi Wang, Fei Xie, Zhibin Quan, Wei Wang, Hao Wang, Yuncong Yao, Wankou Yang, and Satoshi Suzuki. "Siamese Transformer Network: Building an autonomous real-time target tracking system for UAV". In: *Journal of Systems Architecture* 130 (2022), p. 102675.
- [25] Boyu Zhou, Fei Gao, Luqi Wang, Chuhao Liu, and Shaojie Shen. "Robust and efficient quadrotor trajectory generation for fast autonomous flight". In: *IEEE Robotics and Automation Letters* 4.4 (2019), pp. 3529–3536.
- [26] Pete Florence, John Carter, and Russ Tedrake. "Integrated perception and control at high speed: Evaluating collision avoidance maneuvers without maps". In: *Algorithmic Foundations of Robotics XII: Proceedings of the Twelfth Workshop on the Algorithmic Foundations of Robotics*. Springer. 2020, pp. 304–319.
- [27] Yunlong Song, Elia Kaufmann, Leonard Bauersfeld, Antonio Loquercio, and Davide Scaramuzza. *Dodge-Drone: Vision-based Agile Drone Flight (ICRA 2022 Competition)*. [Accessed on 12-02-2024]. 2022. URL: <https://uzh-rpg.github.io/icra2022-dodgedrone/>.
- [28] Yunlong Song, Selim Naji, Elia Kaufmann, Antonio Loquercio, and Davide Scaramuzza. "Flightmare: A Flexible Quadrotor Simulator". In: *Conference on Robot Learning*. 2020.
- [29] Enze Xie, Wenhai Wang, Zhiding Yu, Anima Anandkumar, Jose M Alvarez, and Ping Luo. "SegFormer: Simple and Efficient Design for Semantic Segmentation with Transformers". In: *Neural Information Processing Systems (NeurIPS)*. 2021.
- [30] Wenzhe Shi, Jose Caballero, Ferenc Huszár, Johannes Totz, Andrew P. Aitken, Rob Bishop, Daniel Rueckert, and Zehan Wang. "Real-Time Single Image and Video Super-Resolution Using an Efficient Sub-Pixel Convolutional Neural Network". In: *2016 IEEE Conference on Computer Vision and Pattern Recognition (CVPR)*. 2016, pp. 1874–1883. DOI: 10.1109/CVPR.2016.207.
- [31] Will Constable, Xu Zhao, Victor Bittorf, Eric Christoffersen, Taylor Robie, Eric Han, Peng Wu, Nick Korovaiko, Jason Ansel, Orion Reblitz-Richardson, and Soumith Chintala. *TorchBench: A collection of open source benchmarks for PyTorch performance and usability evaluation*. Sept. 2020. URL: <https://github.com/pytorch/benchmark>.
- [32] Yuezhan Tao, Yuwei Wu, Beiming Li, Fernando Cladera, Alex Zhou, Dinesh Thakur, and Vijay Kumar. "Seer: Safe efficient exploration for aerial robots using learning to predict information gain". In: *2023 IEEE International Conference on Robotics and Automation (ICRA)*. IEEE. 2023, pp. 1235–1241.
- [33] *GitHub - KumarRobotics/kr_mav_control: Code for quadrotor control — github.com*. https://github.com/KumarRobotics/kr_mav_control. [Accessed 14-03-2024].
- [34] Lorenz Meier, Dominik Honegger, and Marc Pollefeys. "PX4: A node-based multithreaded open source robotics framework for deeply embedded platforms". In: *2015 IEEE international conference on robotics and automation (ICRA)*. IEEE. 2015, pp. 6235–6240.
- [35] Hang Yu, Guido CH E de Croon, and Christophe De Wagter. "AvoidBench: A high-fidelity vision-based obstacle avoidance benchmarking suite for multi-rotors". In: *2023 IEEE International Conference on Robotics and Automation (ICRA)*. IEEE. 2023, pp. 9183–9189.